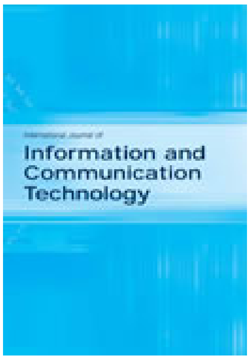

International Journal of Information and Communication Technology

ISSN online: 1741-8070 - ISSN print: 1466-6642
https://www.inderscience.com/ijict

Simulation and visualisation for a wind power prediction model based on structural attention LSTM and environmental correction

Yunuo Chen

DOI: 10.1504/IJICT.2025.10071554

Article History:

Received:	14 March 2025
Last revised:	07 April 2025
Accepted:	07 April 2025
Published online:	18 June 2025

Simulation and visualisation for a wind power prediction model based on structural attention LSTM and environmental correction

Yunuo Chen

College of Electrical Engineering and New Energy,
China Three Gorges University,
Yichang, Hubei – 443002, China
Email: cytusyn@foxmail.com

Abstract: With the increasing share of renewable energy, its volatility poses challenges to grid dispatching, making wind power prediction crucial. Existing methods mainly include point forecasting and probabilistic forecasting, but the former struggles to capture fluctuations, while the latter lacks reasonable scenario generation for grid integration. Additionally, current approaches fail to fully utilise wind farm spatial structures and environmental factors, limiting prediction accuracy and generalisation. To address this, this paper proposes a scenario generation model (SLEP) based on structural attention LSTM and environmental correction. SLEP integrates temporal wind power characteristics, turbine spatial structures, and environmental factors, built upon TimeGAN. SA-LSTM combines a graph convolutional network (GCN) with LSTM to capture spatiotemporal wind power features, while the environmental correction module (ERM) employs cross-attention to embed environmental variables, improving sample adaptability. Experiments show that SLEP outperforms existing methods in accuracy, scenario diversity, and environmental adaptability, providing reliable support for grid dispatching.

Keywords: wind power forecasting; deep generative model; structural attention LSTM; environmental correction; scenario generation.

Reference to this paper should be made as follows: Chen, Y. (2025) ‘Simulation and visualisation for a wind power prediction model based on structural attention LSTM and environmental correction’, *Int. J. Information and Communication Technology*, Vol. 26, No. 20, pp.56–74.

Biographical notes: Yunuo Chen is a Master’s candidate. He graduated from China Three Gorges University in 2025. His research interest is Renewable energy power output scenario generation.

1 Introduction

With the global energy transition and increasing awareness of environmental protection, the share of renewable energy in power systems continues to rise (Yang and Pan, 2025; Li et al., 2022; Breyer et al., 2022). In particular, wind power, as a clean and renewable energy source, has been experiencing continuous growth in both installed capacity and power generation share (Pan et al., 2024; Chen et al., 2022; Siram et al., 2022). However, due to the inherent intermittency and volatility of wind energy, the uncertainty in wind power output poses significant challenges to the safe and stable operation of the power grid (Medina et al., 2022; Ullah et al., 2024; Malik et al., 2024). Grid dispatching and reserve capacity planning urgently require high-precision wind power forecasting, while the uncertainty of wind power also introduces risks in electricity market transactions (Lu et al., 2024; Wang et al., 2022a). Therefore, improving the accuracy of wind power forecasting and generating representative multi-scenario predictions have become key issues that need to be addressed in the field of renewable energy (Zheng et al., 2025; Liu et al., 2024a).

Currently, wind power forecasting methods can be broadly categorised into point forecasting and probabilistic forecasting. Point forecasting methods (Zhang et al., 2023a; Yan et al., 2022; Ye et al., 2022) are computationally simple and easy to implement, but they provide only a single deterministic value, failing to accurately capture the volatility and uncertainty of wind power output, which often leads to deviations from actual conditions (Tsai et al., 2023). On the other hand, probabilistic forecasting methods (Xie et al., 2023; Bazionis et al., 2022; Fan et al., 2023) construct power distribution models to characterise the stochastic nature of wind power to some extent. However, in practical applications, most models focus on improving forecasting accuracy while neglecting the comprehensive utilisation of complex spatial structure information and environmental factors within wind farms (Eikeland et al., 2022). Particularly in grid dispatching, scheduling departments rely on representative multi-scenario forecasts to develop more reasonable scheduling strategies and reserve capacity plans, yet existing methods have limitations in scenario generation (Wang et al., 2022b). Moreover, some approaches lack a holistic consideration of the mutual influence among wind turbines during modelling, leading to insufficient capture of global dynamic characteristics (Wang et al., 2022c). Hence, there is an urgent need for a scenario generation method that comprehensively integrates temporal characteristics, spatial structures, and environmental information to enhance forecasting accuracy, generalisation ability, and scenario diversity, thereby meeting the practical demands of mid- to long-term wind power forecasting and grid dispatch optimisation.

To address the shortcomings of existing methods in leveraging spatial structure and environmental factors, this paper proposes a wind power scenario generation model based on structural attention LSTM and environmental correction (SLEP). In its design, SLEP first constructs a topological graph of wind turbines and employs a graph convolutional network (GCN) (Xu et al., 2023; Wang et al., 2023) to capture local spatial correlations. Then, a structural attention LSTM (SA-LSTM) is utilised to fuse static turbine characteristics with dynamic power data. The core concept of SA-LSTM is to fully exploit the interdependencies among wind turbines within a wind farm while using LSTM to capture the evolving power patterns over time, thereby obtaining a global spatiotemporal feature representation. This structure allows the model to achieve fine-grained modelling of power variations in individual turbines while comprehensively considering the interactions among different turbines in a wind farm, effectively addressing the limitations of traditional point and probabilistic forecasting methods in capturing spatial information. Furthermore, during the adversarial training process of the generator and discriminator, SLEP introduces an environmental correction module (ERM), which employs a cross-attention mechanism to embed key environmental variables such as wind speed, wind direction, and temperature into the generation process. This ensures that the generated samples not only reflect the temporal characteristics of wind power but also better adapt to wind condition variations under different environmental conditions. To prevent excessive fusion of generated features with environmental information, which could reduce sample diversity, an orthogonal loss function is designed to constrain the directional relationship between generated features and environmental features, ensuring that the model retains sufficient power variation and diversity while being constrained by environmental conditions. Through this multi-mechanism design, the SLEP model not only achieves deep integration of spatiotemporal and environmental information in data representation but also enhances the authenticity and diversity of generated samples through multi-loss function optimisation in adversarial training.

In summary, the main contributions of this paper are as follows:

1. A novel structural attention LSTM (SA-LSTM) is proposed to fully capture spatial correlations and temporal characteristics among wind turbines.
2. An ERM is designed, which effectively integrates environmental factors such as wind speed and wind direction using a cross-attention mechanism and maintains the diversity of generated samples through an orthogonal loss constraint.
3. A deep generative adversarial network (GAN)-based wind power scenario generation model (SLEP) is developed, addressing the shortcomings of existing methods in forecasting accuracy, scenario generation, and integration with grid dispatching.

2 Related work

2.1 Methods based on point forecasting

Wind power forecasting is crucial for grid dispatching and renewable energy integration. Point forecasting methods are widely applied due to their computational efficiency and ease of implementation. Zhu et al. (2023) proposed a multi-objective upper-lower bound and point estimation (MOULPE) model, which constructs a dual-output neural network (NN) to directly estimate prediction intervals and uses the median as the point forecast value. This method optimises prediction performance through an improved genetic algorithm, demonstrating low prediction errors across multiple wind power datasets. However, its applicability to different machine learning (ML) methods has been insufficiently explored. To address this limitation, Karaman (2023) investigated artificial neural networks (ANN), recurrent neural networks (RNN), convolutional neural networks (CNN), and long short-term memory (LSTM) networks for wind power forecasting, incorporating both internal wind speed and direction as well as external meteorological data. Their results confirmed that LSTM is suitable for wind power forecasting, though the method did not consider the impact of large-scale climate patterns on wind power. Yang et al. (2024) further studied seasonal wind energy forecasting by leveraging climate model predictions to forecast wind power variations several months in advance based on the El Niño-Southern Oscillation (ENSO) in the US Great Plains region. Although this approach performed well for long-term forecasting, it still required more precise models for short-term forecasting. For short-term wind power prediction, Chang and Niu (2024) proposed an LSTNet model based on secondary decomposition, using CEEMDAN and VMD to pre-process wind power time series, combined with kernel density estimation

(KDE) to provide prediction intervals. Experimental results showed that this method outperformed traditional approaches in forecasting accuracy, but it overlooked the spatial structural information among wind turbines. Additionally, Wang et al. (2024b) studied the impact of numerical weather prediction (NWP) errors on wind power forecasting and proposed a ResNet-GRU-based wind speed correction model to improve wind speed prediction accuracy. Subsequently, they applied a CNN-LSTM model with an attention mechanism for short-term wind power forecasting, optimising model parameters to enhance prediction accuracy. However, this approach remained limited to point forecasting and failed to generate diverse prediction scenarios to support grid dispatching decisions.

The above methods have achieved certain improvements in wind power forecasting accuracy, but they share some common limitations. First, most of them focus solely on point forecasting and lack the ability to generate diverse scenarios, which is essential for grid dispatching. Second, they fail to adequately model the spatial structures among wind turbines, limiting their ability to capture complex spatiotemporal dependencies.

2.2 Methods based on probabilistic forecasting

Due to the stochastic and intermittent nature of wind power, point forecasting is often insufficient for grid dispatching. Therefore, probabilistic forecasting methods have been widely studied to quantify the uncertainty in wind power generation and improve scheduling reliability. Chaouch (2023) employed a conditional quantile regression method for wind speed probabilistic forecasting, providing hourly prediction intervals that facilitate risk management. However, this method mainly focused on wind speed rather than directly predicting wind power output. To enhance the accuracy of probabilistic wind power forecasting, Zhu et al. (2022) proposed a probabilistic forecasting method integrating variational mode decomposition (VMD), singular spectrum analysis (SSA), convolutional neural networks (CNN), and bidirectional gated recurrent units (BGRU). This approach uses VMD-SSA to reduce data complexity, extracts temporal features with CNN-BGRU, and generates probabilistic prediction intervals through quantile regression (QR) and kernel density estimation (KDE). Experimental results demonstrated that this method provides reliable probabilistic distributions while maintaining high forecasting accuracy, but its sensitivity to anomalous data affects stability. Regarding data pre-processing, Zhang et al. (2023b) combined isolation forest (IF), wavelet transform (WT), and categorical boosting (CatBoost) for probabilistic wind power forecasting. This method first removes outlier data points, then applies wavelet transform for frequency decomposition, and utilises CatBoost to extract nonlinear features, ultimately generating prediction intervals through quantile regression. Experiments showed that this method achieved strong generalisation ability and accuracy across multiple wind power datasets, though its high computational complexity limited real-time applications. To enhance model generalisation, Deng et al. (2024) proposed a Bayesian LSTM (BNN-LSTM), incorporating prior distributions on LSTM layer weights to improve adaptability to wind power fluctuations. This method combines a temporal convolutional neural network (TCNN) for feature extraction and mutual information entropy for dimensionality reduction of meteorological data, improving computational efficiency. Experimental results indicated that BNN-LSTM outperformed Bayesian neural networks (BNN) and the latest temporal fusion transformer (TFT) in probabilistic forecasting accuracy. However, the high computational cost of Bayesian inference constrained its practical applicability. Bazionis and Georgilakis (2021) reviewed probabilistic wind power forecasting methods, highlighting the extensive application of multi-model fusion and deep learning in this field, emphasising that combining statistical and machine learning approaches can improve forecasting accuracy and stability.

The above probabilistic forecasting methods have made significant progress in improving the quantification of uncertainty and accuracy in wind power prediction. However, they share some common limitations. On one hand, most methods involve high computational complexity, making them unsuitable for real-time applications; on the other hand, their sensitivity to anomalous data and limited model stability remain key challenges affecting practical usability.

Compared to existing methods that focus solely on point or probabilistic forecasting, the proposed SLEP model introduces a novel integration of spatial structure, temporal dynamics, and environmental factors for wind power scenario generation. While structural attention mechanisms have been explored in fields like traffic forecasting, those typically rely on fixed physical networks. In contrast, our SA-LSTM constructs a dynamic topological graph based on turbine output similarity, capturing flexible, data-driven spatial dependencies unique to wind farms. Combined with the ERM module – which embeds environmental variables via cross-attention while preserving scenario diversity – SLEP offers a more adaptive and realistic approach to wind power forecasting, distinguishing itself from existing models in both structure and application.

3 Proposed method

To address the challenges in long-term wind power scenario generation, particularly the inability to model spatial structures and environmental features effectively, we propose a wind power scenario generation model, scenario-based long-term electricity prediction (SLEP). SLEP is based on TimeGAN and incorporates a structural attention LSTM (SA-LSTM) and an ERM to enhance forecasting performance. The overall framework of the SLEP model is illustrated in Figure 1.

SLEP utilises an embedding network and a recovery network to achieve deep representation and reconstruction of the original wind turbine data, including static features S and dynamic features X_t. Additionally, environmental features E_t are integrated into the adversarial learning process of the generator and discriminator, enabling the generation of long-sequence scenarios that realistically reflect the temporal variations of wind power and environmental conditions. First, the static features S and dynamic features X_t are fed into the SA-LSTM of the embedding network for feature extraction, yielding static hidden features h_S and dynamic hidden features h_t. The recovery network then performs an inverse mapping on $\{h_S, h_t\}$, reconstructing $\{\tilde{S}, \tilde{X}_t\}$ for reconstruction error evaluation. During the generation phase, random noise inputs $\{z_S, z_t\}$ are combined with environmental features E_t and processed by the generator to produce $\{\hat{h}_S, \hat{h}_t\}$. Finally, at the discriminator stage, the ERM refines the generated dynamic noise features to enhance the adaptation of generated scenarios to real wind conditions. These generated samples are then used in adversarial training along with real samples $\{S, X_t\}$.

Figure 1 The framework of the scenario-based long-term electricity prediction (SLEP) model (see online version for colours)

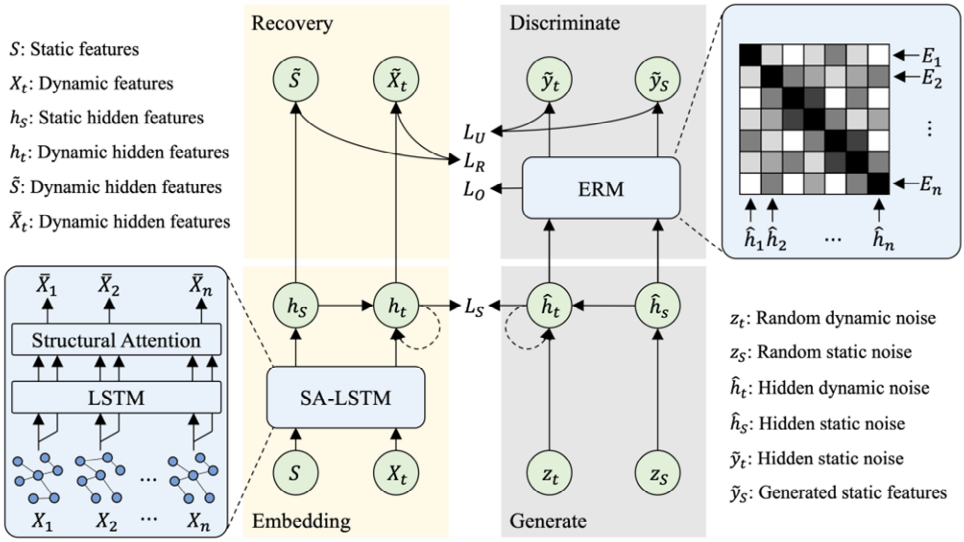

3.1 Structural attention LSTM

To fully capture the structural correlations among wind turbines and the temporal characteristics of wind power output, we design a structural attention long-short-term memory (SA-LSTM) module within the embedding network. As shown in Figure 2, SA-LSTM adopts an integrated architecture that first utilises GCNs to extract spatial dependencies from the topological graph of wind turbines, and then applies an LSTM network to model temporal dynamics. The spatial features extracted by the GCN are fused with time-series data and further enhanced through a structural attention mechanism. This attention mechanism dynamically assigns weights based on the topological positions of turbines and their temporal relevance, thereby weighting the interactions among turbines accordingly.

First, the static features S corresponding to wind turbine identifiers are treated as node information, while the wind power sequence X_t is regarded as the node feature that changes over time. A topological graph G_t is constructed based on the similarity of power output among turbines. In this topology, A represents the adjacency matrix, and the edges between nodes are established based on the similarity of historical power output patterns. The edge weights are computed using a Gaussian kernel function applied to the correlation distances between pairs of turbines, and D represents the degree matrix. At each time step t, it is necessary to integrate power information from neighbouring turbines to obtain a global structural representation, which is then combined with temporal information to better capture the spatial and temporal dynamics of wind power. Specifically, graph convolution is first applied to X_t over the graph structure to obtain the graph embedding representation H_t. The process of graph convolution is formulated as equation (1):

$$H_t = \sigma\left(D^{-\frac{1}{2}} A D^{-\frac{1}{2}} X_t W_t\right) \tag{1}$$

where σ represents the ReLU activation function, and W_t is a trainable parameter matrix. This approach extracts local spatial correlations from the graph structure, helping the model understand the mutual influence among wind turbines within a wind farm. Subsequently, to obtain higher-level feature representations, H_t is further mapped into a global representation space, as formulated in equation (2):

$$F_t = \sigma\left(W_t' H_t\right) \tag{2}$$

where W_t' is another trainable parameter matrix. Then, F_t is fed into the LSTM to capture the evolving power patterns over time, yielding the LSTM output F_t'.

Figure 2 The process flow of structural attention LSTM (see online version for colours)

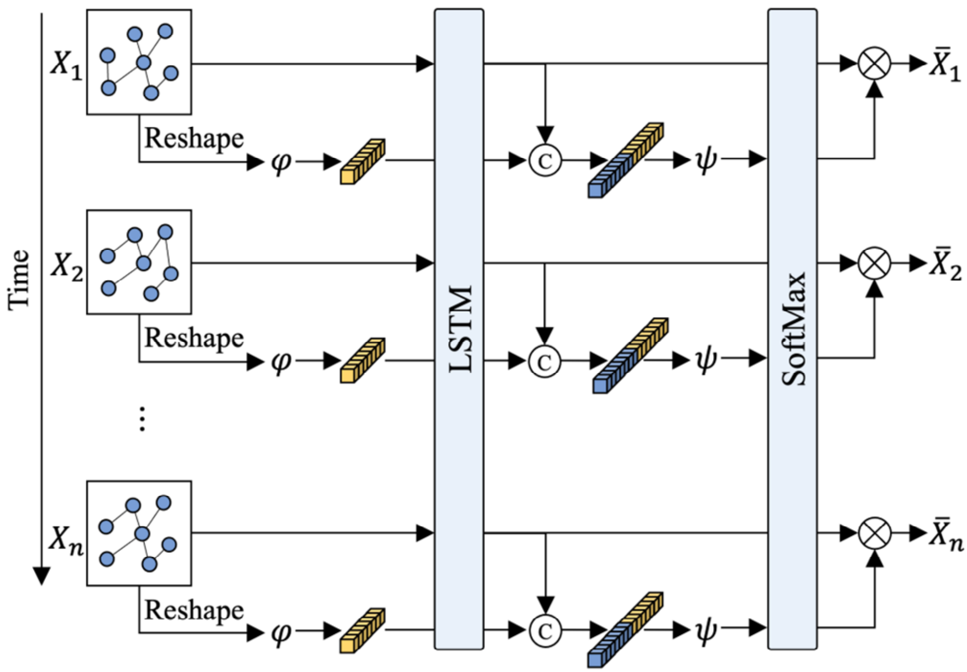

Since the importance of different turbines in the topological structure varies and may change over time, a structural attention mechanism is introduced after extracting global features. First, the topological graph G_t is reshaped according to turbine indices, and a mapping function ϕ is applied to obtain the structural features S_t. The structural features S_t are then concatenated with the temporal features F_t', followed by a mapping function ψ and a softmax activation to generate the structural attention coefficients. The entire process is formulated in equation (3):

$$\alpha_t = \text{softmax}\left(\psi\left(ReLU\left(\phi\left(Reshape\left(G_t\right)\right)\right) \Vert F_t'\right)\right) \tag{3}$$

where || represents the concatenation operation, *ReLU* is the activation function, and softmax is used to normalise the output vector. Through this step, the model can adaptively focus on the most relevant turbine structural information at different time steps and dynamically assign attention weights for each time step, thereby highlighting key interactions among turbines. Finally, the attention coefficients are multiplied element-wise with the temporal features to obtain the final output of SA-LSTM, expressed as $\bar{X}_t = \alpha_t \cdot F_t'$.

3.2 Environmental rectification module

At the discriminator stage, to further enhance the adaptation of generated samples to actual wind conditions, we design an ERM that computes cross-attention between the hidden dynamic noise $\hat{h}_t$ and environmental features E_t. Here, E_t represents meteorological factors closely related to wind power generation, including wind speed, wind direction, temperature, and atmospheric pressure, embedded as feature representations. During adversarial training, E_t serves as both a reference condition for the discriminator to distinguish real from fake samples and as guidance in the generator to direct the generation of dynamic noise.

Specifically, the discriminator first encodes E_t as the query, while $\hat{h}_t$ undergoes multi-head or single-head cross-attention computation using trainable parameters W_Q, W_K, and W_V, resulting in the corrected $\hat{h}_t$. This attention process is formulated in equation (4):

$$\hat{h}_t = \text{softmax}\left(\frac{W_Q E_t \left(W_K \hat{h}_t\right)}{\sqrt{d_k}}\right) W_V \hat{h}_t \tag{4}$$

where W_Q maps E_t into the query space, W_K maps $\hat{h}_t$ into the key space, and W_V maps $\hat{h}_t$ into the value space. The term $\sqrt{d_k}$ is a scaling factor used to balance the magnitude of the dot product. Compared to directly concatenating E_t to the discriminator input, ERM embeds environmental features through an attention mechanism, allowing the discriminator to flexibly learn the influence of different environmental variables on noise feature correction, thereby achieving more precise adversarial learning.

On this basis, to prevent excessive alignment between the generated features and environmental features while ensuring that the generated features remain constrained by environmental factors, we aim to preserve the diversity of wind power sequence variations. This enables the model to better adapt to various wind conditions that may occur in mid- to long-term power forecasting scenarios. To achieve this, we introduce an orthogonal loss to constrain the directional relationship between $\hat{h}_t$ and E_t. This additional mechanism enhances the utilisation of environmental information beyond the attention mechanism. By maintaining a certain degree of orthogonality between their vector directions, the model avoids excessive dependence on environmental features during training, thereby preserving essential power variability.

3.3 Loss functions

During the training process, to ensure the quality of generated samples while maintaining environmental consistency and the accuracy of power time series, we employ four loss functions for joint optimisation. The first is the supervised loss L_S, which measures the difference between the dynamic hidden features h_t output by the embedding network and the dynamic hidden features $\hat{h}_t$ generated by the generator network, as formulated in equation (5):

$$L_S = \mathbb{E}_{S,X_1:T}\left[\sum_t \left\|h_t - \hat{h}_t\right\|_2\right] \tag{5}$$

The supervised loss L_S constrains the real hidden features and generated hidden features, enabling the generator network to learn the true distribution of wind power in the temporal dimension. This ensures that the generated features maintain consistency with real features in terms of dynamic trends. The second loss function is the unsupervised adversarial loss L_U, which measures the discriminator's ability to distinguish between real samples $\{S, X_t\}$ and generated samples $\{\hat{h}_S, \hat{h}_t\}$, as formulated in Equation (6):

$$L_U = \mathbb{E}_{S,X_1\cdot T}\left[\log y_S + \sum_t \log y_t\right] + \mathbb{E}_{S,X_1:T}\left[\log(1-\tilde{y}_S) + \sum_t \log(1-\tilde{y}_t)\right] \tag{6}$$

where y_S and y_t represent the discriminator's classification results for the real static and dynamic features, respectively, while $\tilde{y}_S$ and $\tilde{y}_t$ denote the discriminator's classification results for the generated features. This loss function enhances the realism and diversity of generated samples through the adversarial interplay between the discriminator and the generator, enabling the model to learn a generation pattern that closely aligns with the actual wind power distribution. Next, the reconstruction loss L_R evaluates the consistency between the original features $\{S, X_t\}$ and the output of the recovery network $\{\tilde{S}, \tilde{X}_t\}$, as formulated in equation (7):

$$L_R = \mathbb{E}_{S,X_1:T}\left[\left\|S - \tilde{S}\right\|_2 + \sum_t \left\|X_t - \tilde{X}_t\right\|_2\right] \tag{7}$$

The reconstruction loss L_R ensures that the embedding network and the recovery network accurately represent and reconstruct wind power time series data and turbine static information. This prevents the loss of critical features during the embedding or generation process, thereby establishing a stable underlying representation for subsequent adversarial training. Finally, the orthogonal loss L_O is introduced in ERM to constrain the directional relationship between $\hat{h}_t$ and E_t, as formulated in Equation (8):

$$L_O = \sum_n \left\|\frac{\hat{h}_n}{\left\|\hat{h}_n\right\|} \cdot \frac{E_n}{\left\|E_n\right\|}\right\|^2 \tag{8}$$

The orthogonal loss L_O is computed using the normalised inner product to suppress excessive overlap between $\hat{h}_n$ and E_n. This prevents the generated features from losing diversity when incorporating environmental information while ensuring adaptability to the potential variation space of wind power.

4 Experiments

4.1 Dataset and evaluation metrics

The dataset used in this study is collected from a wind farm in northern China, selecting data from seven wind turbines, with each turbine serving as a fundamental data unit. The dataset includes time-series data of wind power, wind speed, wind direction, atmospheric pressure, and humidity. The data sampling resolution is 15 minutes, and each wind turbine contains a total of 2,500 data samples. To ensure the generalisation capability of the model, the data is split in an 8:2 ratio, with the first 2,000 samples used for training and the remaining 500 samples used as a test set. This ensures that the test data is independent of the training process, providing an objective evaluation of the model's actual forecasting performance. To comprehensively assess the predictive ability of the model, we employ two types of error metrics: longitudinal error and transverse error. The longitudinal error measures the numerical deviation of the predicted results, using the mean absolute error (MAE) as the evaluation metric. MAE reflects the average deviation between predicted and actual values, with a smaller MAE indicating higher forecasting accuracy. The transverse error evaluates the temporal consistency between the predicted sequence and actual data, using the correlation coefficient (CC) as the evaluation criterion. A CC value closer to 1 indicates that the predicted sequence closely follows the trend of the actual sequence, accurately capturing the temporal fluctuations of wind power.

4.2 Experimental setup and environment

The experiments were conducted in an Ubuntu 20.04 environment. The hardware configuration includes an Intel Xeon Silver 4210R CPU at 2.40 GHz, an NVIDIA RTX 3090 GPU with 24 GB memory, and 128 GB of RAM. For the software environment, Python 3.8 was used, and deep learning modelling was implemented using PyTorch 1.10. The model training process employed the Adam optimiser with an initial learning rate of 0.001. The learning rate was adjusted using ReduceLROnPlateau with a decay rate of 0.1. The batch size was set to 64, and the maximum number of training epochs was 200. The hidden layer dimension was set to 128, with ReLU as the activation function. Dropout regularisation (0.3) was applied before and after the fully connected layers.

4.3 Results and analysis

4.3.1 Ablation study

To verify the effectiveness of the structural attention LSTM (SA-LSTM) and the ERM in the SLEP model, we designed an ablation study. We conducted comparative analyses by removing SA-LSTM and ERM separately, and the experimental results are presented in Table 1.

From the experimental results, it can be observed that the complete SLEP model achieves the lowest MAE and the highest CC. When SA-LSTM or ERM is removed, the model's performance degrades in both accuracy and trend matching. Specifically, removing SA-LSTM results in an average increase of 1.0%–1.2% in MAE and a decrease of 3%–4% in CC, indicating that SA-LSTM plays a crucial role in spatiotemporal feature extraction. It effectively models the correlations among wind turbines, enhancing both prediction accuracy and trend alignment. When ERM is removed, MAE increases by 0.6%–0.9%, while CC drops by 1.5%–2.2%, demonstrating that the ERM significantly improves the model's adaptability to environmental variations. It effectively reduces prediction bias caused by external environmental changes. Without SA-LSTM, the model cannot fully utilise the spatial topology among turbines and relies solely on LSTM for temporal modelling, leading to increased prediction errors. This is particularly evident during periods of rapid wind condition changes, where the model struggles to capture power fluctuation trends accurately. Additionally, the decline in CC suggests an increased lag in trend matching within the time series. Without ERM, the model's ability to adapt to environmental factors weakens, making it difficult to adjust the power prediction distribution. As a result, prediction errors increase, especially in cases where wind speed and wind direction fluctuate significantly, reducing the accuracy of power fluctuation trend predictions.

Table 1 The impact of SA-LSTM and ERM on the performance of the SLEP model

Unit	*SLEP*		*w/o SA-LSTM*		*w/o ERM*	
	MAE (%)	*CC (%)*	*MAE (%)*	*CC (%)*	*MAE (%)*	*CC (%)*
1	12.53	77.89	13.62	74.15	13.21	75.88
2	14.43	74.81	15.29	71.64	14.98	73.12
3	13.87	79.21	14.92	76.08	14.54	77.31
4	14.65	75.33	15.72	71.92	15.28	73.65
5	14.72	77.39	15.84	74.26	15.36	75.84
6	14.18	73.88	15.30	71.02	14.96	72.44
7	14.87	71.33	15.92	68.51	15.48	69.74

4.3.2 Analysis of power forecasting and scenario generation results

To visually demonstrate the predictive capability of the SLEP model, we selected the forecasting results of seven wind turbines over a 20-day period and compared them with actual wind power outputs. The results are shown in Figure 3. The red curve represents the model's predicted values, while the green curve indicates the actual wind power output.

From the results, SLEP effectively captures the overall temporal variations of wind power, particularly in regions with significant fluctuations in power levels, where the predicted values closely follow the actual data. For most wind turbines, the prediction curves accurately capture the primary peak and valley characteristics of wind power, and the high CC indicates strong trend-fitting ability in the time series. However, in certain periods of rapid power fluctuations, the model exhibits some degree of lag, primarily reflected in a phase shift between the predicted and actual curves. Additionally, in certain low-power regions, the predicted values are slightly overestimated, which may be due to the complex influence of environmental factors such as wind speed and wind direction, leading to limitations in the model's generalisation capability. Overall, SLEP accurately predicts the temporal characteristics of wind power and demonstrates stable forecasting performance across different turbines. This indicates that the model effectively integrates spatial information of wind turbines and environmental features, enhancing its ability to capture power fluctuation trends and providing reliable data support for wind power forecasting and grid dispatching.

Figure 3 Wind power forecasting visualisation of the SLEP model (see online version for colours)

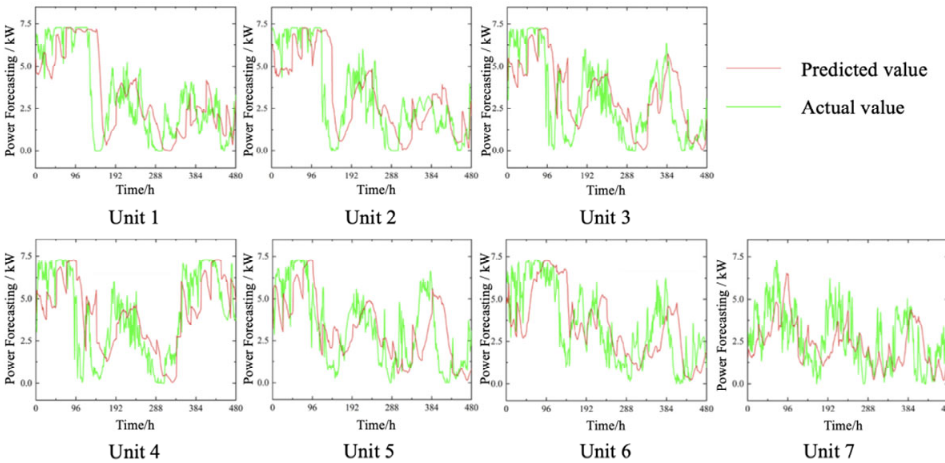

To further evaluate the capability of the SLEP model in wind power scenario generation, we generated 50 wind power output scenarios based on the forecasting results. A subset of scenarios for seven wind turbines over a three-day period (72 time steps) is illustrated in Figure 4. In the figure, the red curve represents the model's predicted values, the green curve denotes the actual wind power, and the multiple semi-transparent background curves represent various possible wind power scenarios generated by the model.

Figure 4 Wind power scenario generation visualisation of the SLEP model (see online version for colours)

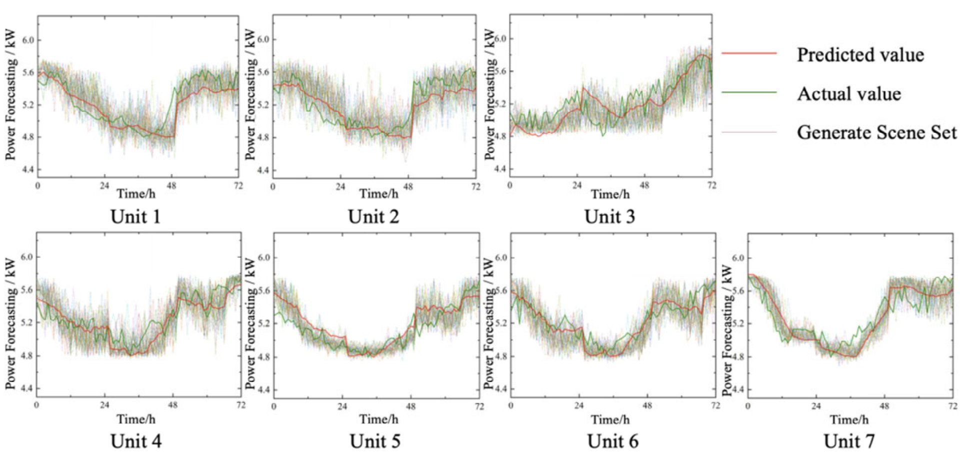

From the figure, it can be observed that the scenario set generated by SLEP effectively covers the variation range of actual wind power while exhibiting a reasonable distribution pattern that reflects the possible fluctuations of wind power at different time steps. This demonstrates that SLEP not only provides a single predicted value but also captures the uncertainty of wind power, offering more diverse and informative forecasting results for grid dispatching. In periods where wind power fluctuations are relatively stable, the predicted curves closely align with the actual curves, and the generated scenario set exhibits low dispersion, indicating that the model performs accurately under steady wind conditions. In contrast, during periods of significant wind power fluctuations, the scenario set displays greater divergence, encompassing various possible wind power outputs. This highlights the model's capability to reasonably model the uncertainty of power generation.

Finally, to validate the spatial consistency of the wind power scenarios generated by SLEP, we conducted a Spearman spatial correlation analysis on 50 generated wind power scenarios across seven wind turbines. The results are illustrated in Figure 5. The boxplot presents the distribution of CCs across different turbine pairs, with red circles representing the mean values and black diamond points indicating outliers.

Figure 5 Spearman spatial CCs of the SLEP model (see online version for colours)

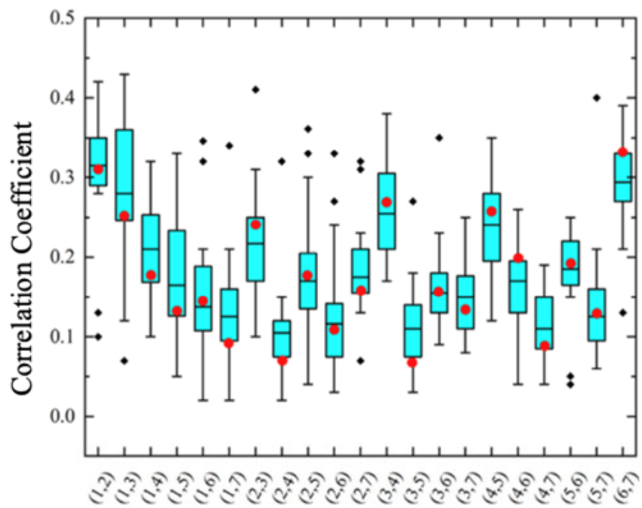

From the analysis results, it can be observed that the correlation between different wind turbines varies significantly. Some turbine pairs exhibit high Spearman CCs, indicating strong spatial consistency in power fluctuations, which may be influenced by similar wind resources or geographic proximity. Conversely, turbine pairs with lower CCs suggest distinct wind power output patterns, possibly due to differences in wind direction, wind speed, or local terrain effects. Additionally, for certain turbine pairs, the distribution of CCs appears more dispersed, implying that the range of fluctuations across different generated scenarios is relatively large. This reflects the model's ability to effectively capture the uncertainty in wind power generation. Moreover, the presence of outliers suggests that specific scenarios may be influenced by unique wind conditions or random noise, further confirming that the SLEP-generated scenario set exhibits strong diversity.

4.3.3 Comparative experiments

To evaluate the forecasting performance of different methods, we compared the proposed method with three existing LSTM-based wind power forecasting approaches: MTTFA-LSTM (Liu et al., 2024b), SWLSTM (Wang et al., 2024a), and wavelet-LSTM (Liu and Zhou, 2024). The results are shown in Figure 6.

Figure 6 Performance comparison between the proposed SLEP model and existing methods (see online version for colours)

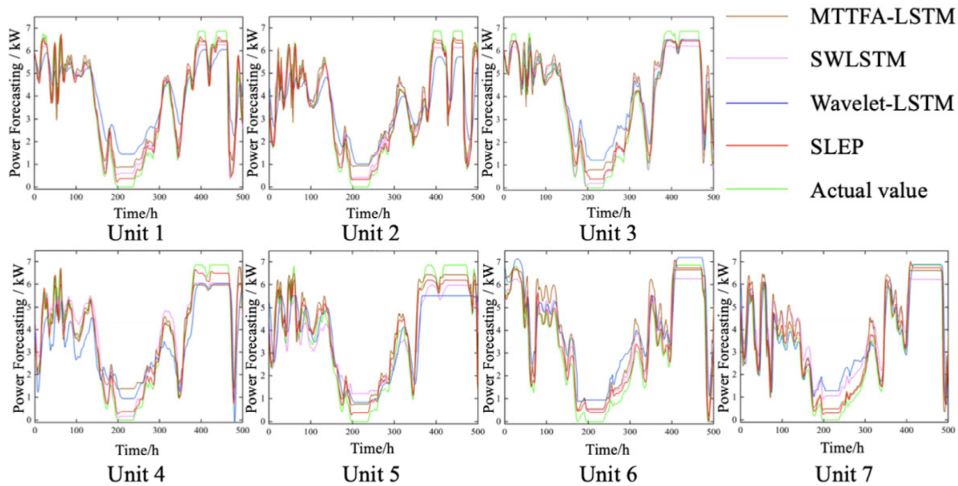

From the results, it can be observed that the prediction curves of SLEP for the seven wind turbines are closer to the actual values, with an overall trend that aligns well with actual wind power variations. In contrast, wavelet-LSTM exhibits significant deviations at certain time points, particularly in regions of abrupt wind power changes, where its predictions show noticeable lag. This is because wavelet-LSTM primarily relies on wavelet decomposition for data denoising but struggles to adapt to rapid fluctuations in complex time series, leading to higher prediction errors during short-term power surges. SWLSTM produces relatively smooth prediction curves for most time periods; however, its prediction accuracy decreases during periods of severe wind power fluctuations, indicating limitations in capturing the nonlinear dynamic characteristics of wind power. Additionally, MTTFA-LSTM, which integrates multi-task learning and attention mechanisms, achieves higher prediction accuracy for some turbines but still struggles with delayed responses to power surges across multiple turbines. This suggests that its generalisation capability remains limited under complex wind conditions. In comparison, SLEP integrates the structural attention LSTM (SA-LSTM) and the ERM, significantly enhancing the spatiotemporal modelling capability of wind power forecasting. SA-LSTM constructs the topological relationships among wind turbines, improving the model's ability to capture spatial distribution characteristics within a wind farm, thereby allowing predictions to more accurately reflect interactions between turbines. ERM utilises environmental features for correction, reducing prediction biases caused by meteorological variations such as wind speed and wind direction, thereby improving the stability and adaptability of the predictions. Compared to other methods, SLEP not only maintains responsiveness to short-term power surges but also improves overall trend matching, resulting in more stable predictions that align with the spatiotemporal evolution patterns of actual wind power.

To further evaluate the generalisation capability of the proposed method, we tested its effectiveness on another photovoltaic power generation dataset and conducted a comparative analysis with other approaches. The comparison results are shown in Figure 7. This dataset was collected from a photovoltaic power plant located in northwestern China. Similar to the previous setup, we selected seven generation units from the plant and compared the proposed model against several existing methods.

Figure 7 Performance comparison between the proposed SLEP model and existing methods on another photovoltaic power generation dataset (see online version for colours)

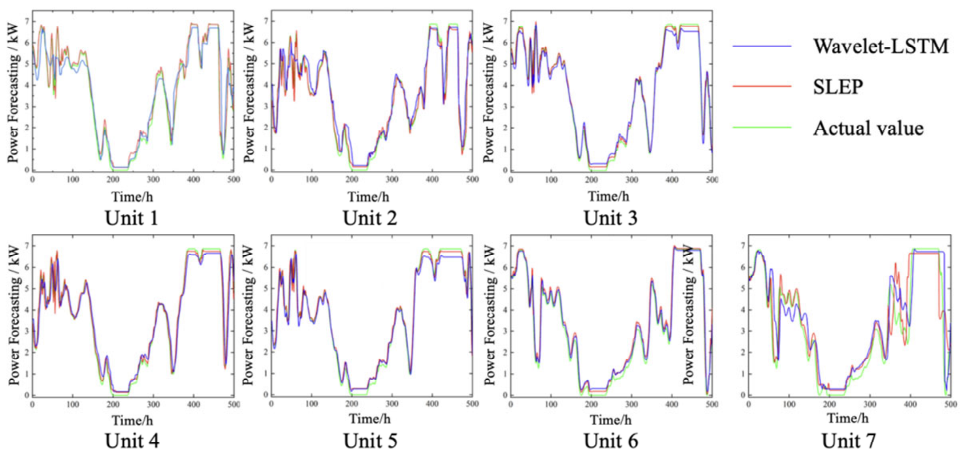

As shown in the figure, SLEP demonstrates higher prediction accuracy across most generation units, with its forecasting curves more closely fitting the actual values. It more accurately captures the trends and fluctuations in power output. In regions with sudden changes or intense variability, SLEP exhibits better responsiveness compared to wavelet-LSTM, highlighting its stronger capability in modelling dynamic features. This indicates that the proposed model is not only effective for wind power forecasting but also shows good generalisation performance in other renewable energy scenarios such as photovoltaic power generation.

5 Conclusions

To address the issues of low accuracy in mid- to long-term wind power forecasting, insufficient scenario generation capability, and weak environmental adaptability, this paper proposes a wind power scenario generation model based on structural attention LSTM (SA-LSTM) and an ERM, referred to as SLEP. By integrating the spatial topological relationships of wind turbines, temporal features, and environmental factors, the model improves both the accuracy and diversity of wind power predictions, providing more reliable data support for grid dispatching and renewable energy integration. Experimental results demonstrate that SLEP outperforms existing methods in terms of prediction accuracy, trend alignment, and scenario generation capability. SA-LSTM, by incorporating GCNs with LSTM, enhances the model's ability to capture spatial correlations among wind turbines, ensuring that predictions more accurately reflect interactions between different turbines. ERM employs a cross-attention mechanism to integrate key environmental variables such as wind speed, wind direction, and temperature while introducing an orthogonal loss function to regulate the relationship between environmental and power features. This effectively reduces the impact of environmental variations on prediction accuracy, improving the realism and diversity of generated scenarios. Moreover, in comparative experiments, SLEP achieved lower prediction errors, higher CCs across multiple wind turbines, and stronger responsiveness to sudden power fluctuations, demonstrating superior generalisation performance and environmental adaptability.

Despite the promising results of SLEP in wind power scenario generation, certain limitations remain that warrant further investigation. First, the model exhibits noticeable prediction lag during periods of rapid and extreme wind power fluctuations. This is primarily due to the inherent limitations of recurrent neural networks like LSTM in capturing highly nonlinear and abrupt temporal patterns, especially under rare or extreme weather events. Although the structural attention mechanism improves temporal awareness, the model's ability to anticipate sudden changes remains constrained by the availability and granularity of training data. Second, while the ERM improves adaptation to meteorological variations, it currently depends on a limited set of environmental variables and assumes a relatively stable correlation between those variables and power output. This could reduce robustness in scenarios involving complex meteorological interactions or sensor noise. A more comprehensive environmental modelling approach, potentially integrating physical models, real-time adaptive mechanisms, or additional meteorological inputs (e.g., turbulence intensity, wind shear), may help address these challenges. Third, the reliance on GANs for scenario generation, although effective, comes with known drawbacks such as training instability, mode collapse, and difficulty in capturing long-term temporal dependencies. This could limit the diversity and realism of the generated scenarios in certain contexts. Exploring alternative generative frameworks, such as variational autoencoders (VAEs), normalising flows, or diffusion-based models, may offer more stable and controllable generation processes. Lastly, the current evaluation is limited to a single wind farm dataset, which may restrict the generalisability of the proposed model to other geographic regions or turbine configurations. Future work should consider training and validating SLEP across multiple wind farms with varying spatial and environmental characteristics to assess its scalability and robustness in broader deployment scenarios.

Declarations

The author declares that it does not have any known interests or personal relationships that could potentially influence the reported work in this paper.

References

Bazionis, I.K. and Georgilakis, P.S. (2021) 'Review of deterministic and probabilistic wind power forecasting: models, methods, and future research', *Electricity*, Vol. 2, No. 1, pp.13–47.

Bazionis, I.K., Karafotis, P.A. and Georgilakis, P.S. (2022) 'A review of short-term wind power probabilistic forecasting and a taxonomy focused on input data', *IET Renewable Power Generation*, Vol. 16, No. 1, pp.77–91.

Breyer, C., Khalili, S., Bogdanov, D., Ram, M., Oyewo, A.S., Aghahosseini, A. and Sovacool, B.K. (2022) 'On the history and future of 100% renewable energy systems research', *IEEE Access*, Vol. 10, pp.78176–78218, https://doi.org/10.1109/ACCESS.2022.3193402.

Chang, C. and Niu, G. (2024) 'Short-term interval prediction of wind power based on quadratic decomposition and BO-LSTNet', in *2024 12th International Conference on Smart Grid and Clean Energy Technologies (ICSGCE)*, IEEE, October, pp.66–72.

Chaouch, M. (2023) 'Probabilistic wind speed forecasting for wind turbine allocation in the power grid', *Energies*, Vol. 16, No. 22, p.7615.

Chen, H., Chen, J., Han, G. and Cui, Q. (2022) 'Winding down the wind power curtailment in China: what made the difference?', *Renewable and Sustainable Energy Reviews*, Vol. 167, p.112725, https://doi.org/10.1016/j.rser.2022.112725.

Deng, Z., Zhang, X., Li, Z., Yang, J., Lv, X., Wu, Q. and Zhu, B. (2024) 'Probabilistic prediction of wind power based on improved Bayesian neural network', *Frontiers in Energy Research*, Vol. 11, p.1309778, https://doi.org/10.3389/fenrg.2023.1309778.

Eikeland, O.F., Hovem, F.D., Olsen, T.E., Chiesa, M. and Bianchi, F.M. (2022) 'Probabilistic forecasts of wind power generation in regions with complex topography using deep learning methods: an Arctic case', *Energy Conversion and Management*, Vol. 10, No. 15, p.100239.

Fan, H., Zhen, Z., Liu, N., Sun, Y., Chang, X., Li, Y. and Mi, Z. (2023) 'Fluctuation pattern recognition based ultra-short-term wind power probabilistic forecasting method', *Energy*, Vol. 266, p.126420, https://doi.org/10.1016/j.energy.2022.126420.

Karaman, Ö.A. (2023) 'Prediction of wind power with machine learning models', *Applied Sciences*, Vol. 13, No. 20, p.11455.

Li, L., Lin, J., Wu, N., Xie, S., Meng, C., Zheng, Y. and Zhao, Y. (2022) 'Review and outlook on the international renewable energy development', *Energy and Built Environment*, Vol. 3, No. 2, pp.139–157.

Liu, X. and Zhou, J. (2024) 'Short-term wind power forecasting based on multivariate/multi-step LSTM with temporal feature attention mechanism', *Applied Soft Computing*, Vol. 150, p.111050, https://doi.org/10.1016/j.asoc.2023.111050.

Liu, Y., Wang, J. and Liu, L. (2024a) 'Physics-informed reinforcement learning for probabilistic wind power forecasting under extreme events', *Applied Energy*, Vol. 376, p.124068.

Liu, Z.H., Wang, C.T., Wei, H.L., Zeng, B., Li, M. and Song, X.P. (2024b) 'A wavelet-LSTM model for short-term wind power forecasting using wind farm SCADA data', *Expert Systems with Applications*, Vol. 247, p.123237, https://doi.org/10.1016/j.eswa.2024.123237.

Lu, P., Zhang, N., Ye, L., Du, E. and Kang, C. (2024) 'Advances in model predictive control for large-scale wind power integration in power systems: a comprehensive review', *Advances in Applied Energy*, Vol. 14, p.100177, https://doi.org/10.1016/j.adapen.2024.100177.

Malik, F.H., Khan, M.W., Rahman, T.U., Ehtisham, M., Faheem, M., Haider, Z.M. and Lehtonen, M. (2024) 'A comprehensive review on voltage stability in wind-integrated power systems', *Energies*, Vol. 17, No. 3, p.644.

Medina, C., Ana, C.R.M. and González, G. (2022) 'Transmission grids to foster high penetration of large-scale variable renewable energy sources – a review of challenges, problems, and solutions', *International Journal of Renewable Energy Research*, Vol. 12, No. 1, pp.146–169.

Pan, H., Feng, W., Ge, J. and Zhang, J. (2024) 'Prediction method of battery remaining life based on CEEMDAN-RF-SED-LSTM neural network', *International Journal of Information and Communication Technology*, Vol. 25, No. 9, pp.1–21.

Siram, O., Sahoo, N. and Saha, U.K. (2022) 'Changing landscape of India's renewable energy and the contribution of wind energy', *Cleaner Engineering and Technology*, Vol. 8, p.100506, https://doi.org/10.1016/j.clet.2022.100506.

Tsai, W.C., Hong, C.M., Tu, C.S., Lin, W.M. and Chen, C.H. (2023) 'A review of modern wind power generation forecasting technologies', *Sustainability*, Vol. 15, No. 14, p.10757.

Ullah, F., Zhang, X., Khan, M., Mastoi, M.S., Munir, H.M., Flah, A. and Said, Y. (2024) 'A comprehensive review of wind power integration and energy storage technologies for modern grid frequency regulation', *Heliyon*, Vol. 10, No. 9, p.e30466.

Wang, C., He, Y., Zhang, H.L. and Ma, P. (2024a) 'Wind power forecasting based on manifold learning and a double-layer SWLSTM model', *Energy*, Vol. 290, p.130076, https://doi.org/10.1016/j.energy.2023.130076.

Wang, S., Liu, H. and Yu, G. (2024b) 'Short-term wind power combination forecasting method based on wind speed correction of numerical weather prediction', *Frontiers in Energy Research*, Vol. 12, p.1391692, https://doi.org/10.3389/fenrg.2024.1391692.

Wang, F., Chen, P., Zhen, Z., Yin, R., Cao, C., Zhang, Y. and Duić, N. (2022a) 'Dynamic spatio-temporal correlation and hierarchical directed graph structure based ultra-short-term wind farm cluster power forecasting method', *Applied Energy*, Vol. 323, p.119579, https://doi.org/10.1016/j.apenergy.2022.119579.

Wang, J., Wang, S., Zeng, B. and Lu, H. (2022b) 'A novel ensemble probabilistic forecasting system for uncertainty in wind speed', *Applied Energy*, Vol. 313, p.118796, https://doi.org/10.1016/j.apenergy.2022.118796.

Wang, K., Zhang, Y., Lin, F., Wang, J. and Zhu, M. (2022c) 'Nonparametric probabilistic forecasting for wind power generation using quadratic spline quantile function and autoregressive recurrent neural network', *IEEE Transactions on Sustainable Energy*, Vol. 13, No. 4, pp.1930–1943.

Wang, H.K., Li, D., Chen, F., Du, J. and Song, K. (2023) 'GCNInformer: a combined deep learning model based on GCN and informer for wind power forecasting', *Energy Science & Engineering*, Vol. 11, No. 10, pp.3836–3854.

Xie, Y., Li, C., Li, M., Liu, F. and Taukenova, M. (2023) 'An overview of deterministic and probabilistic forecasting methods of wind energy', *Iscience*, Vol. 26, No. 1, p.105804.

Xu, H., Zhang, Y., Zhen, Z., Xu, F. and Wang, F. (2023) 'Adaptive feature selection and GCN with optimal graph structure-based ultra-short-term wind farm cluster power forecasting method', *IEEE Transactions on Industry Applications*, Vol. 60, No. 1, pp.1804–1813.

Yan, J., Möhrlen, C., Göçmen, T., Kelly, M., Wessel, A. and Giebel, G. (2022) 'Uncovering wind power forecasting uncertainty sources and their propagation through the whole modelling chain', *Renewable and Sustainable Energy Reviews*, Vol. 165, p.112519, https://doi.org/10.1016/j.rser.2022.112519.

Yang, C. and Pan, H. (2025) 'A time series neural network-based early warning system for thermal power station', *International Journal of Information and Communication Technology*, Vol. 26, No. 4, pp.106–122.

Yang, X., Delworth, T.L., Jia, L., Johnson, N.C., Lu, F. and McHugh, C. (2024) 'Skillful seasonal prediction of wind energy resources in the contiguous United States', *Communications Earth & Environment*, Vol. 5, No. 1, p.313.

Ye, L., Dai, B., Pei, M., Lu, P., Zhao, J., Chen, M. and Wang, B. (2022) 'Combined approach for short-term wind power forecasting based on wave division and Seq2Seq model using deep learning', *IEEE Transactions on Industry Applications*, Vol. 58, No. 2, pp.2586–2596.

Zhang, J., Zhang, R., Zhao, Y., Qiu, J., Bu, S., Zhu, Y. and Li, G. (2023a) 'Deterministic and probabilistic prediction of wind power based on a hybrid intelligent model', *Energies*, Vol. 16, No. 10, p.4237.

Zhang, Z., Li, Z. and Yan, L. (2023b) 'An optimised LSTM algorithm for short-term load forecasting', *International Journal of Information and Communication Technology*, Vol. 22, No. 3, pp.224–239.

Zheng, K., Sun, Z., Song, Y., Zhang, C., Zhang, C., Chang, F. and Fu, X. (2025) 'Stochastic scenario generation methods for uncertainty in wind and photovoltaic power outputs: a comprehensive review', *Energies*, Vol. 18, No. 3, p.503.

Zhu, J., He, Y. and Gao, Z. (2023) 'Wind power interval and point prediction model using neural network based multi-objective optimization', *Energy*, Vol. 283, p.129079, https://doi.org/10.1016/j.energy.2023.129079.

Zhu, Z., Xu, Y., Wu, J., Liu, Y., Guo, J. and Zang, H. (2022) 'Wind power probabilistic forecasting based on combined decomposition and deep learning quantile regression', *Frontiers in Energy Research*, Vol. 10, p.937240, https://doi.org/10.3389/fenrg.2022.937240.